Journal of Translational Medicine

RESEARCH

Open Access

EMB-driven glioblastoma multiforme progression via the MCT4/GPX3 axis: therapeutic inhibition by Ganxintriol A

Bo Cheng[2,4†], Jing Liu[5†], Ling Gao[3], Ziwen Zhu[4], Yang Yang[3], Shangqi Liu[6] and Xiaojin Wu[1*]

Abstract

Background Embigin (EMB) is a transmembrane glycoprotein highly expressed in glioblastoma multiforme (GBM), yet its role in GBM progression remains unclear. In this study, we investigate the function of intracellular EMB in promoting GBM progression and evaluate the effect of Ganxintriol A, a traditional Chinese herbal extract, in GBM treatment.

Methods Bioinformatics datasets were utilized to assess EMB expression and its prognostic value in GBM patients. In vitro experiments such as PCR、western blot,CCK8,transwell,wound healing,clone formation and flow cytometry assays were conducted to examine EMB's biological functions and underlying mechanisms in GBM cell lines. Additionally, we constructed a subcutaneous tumor model in nude mice and evaluated the effect of traditional Chinese medicine extract Ganxintriol A on the progression of GBM through in vivo and in vitro experiments.

Results EMB is highly expressed in GBM and is associated with poor prognosis in GBM patients. EMB overexpression accelerated GBM progression, whereas EMB knockdown had the opposite effect. Further analysis revealed that EMB upregulated epithelial-mesenchymal transition (EMT) and glycolysis while maintaining glutathione (GSH) redox balance by inducing monocarboxylate transporter 4 (MCT4) and glutathione peroxidase 3 (GPX3) expression. Treatment with Ganxintriol A significantly downregulated EMB expression, effectively inhibiting GBM progression both in vitro and in vivo.

Conclusions This study highlights EMB as an independent prognostic biomarker for GBM and reveals a novel mechanism by which EMB drives GBM progression. Additionally, Ganxintriol A is identified as a promising therapeutic candidate for GBM treatment.

†Bo Cheng and Jing Liu are contributed equally to this work.

*Correspondence:
Xiaojin Wu
760020220396@xzhmu.edu.cn
[1] Department of Radiation Oncology, Xuzhou Central Hospital, the Affiliated Xuzhou Clinical College of Xuzhou Medical University, 199 Jiefang South Road, Xuzhou 221000, China
[2] Department of Psychiatry, The Affiliated Xuzhou Eastern Hospital of Xuzhou Medical University, 379 Tongshan Road, Xuzhou 221000, China
[3] Department of Pharmacy, The Affiliated Huaihai Hospital of Xuzhou Medical University, The 71st Group Army Hospital of CPLA Army, 226 Tongshan Road, Xuzhou 221000, China
[4] Department of Neurology, Tongji Hospital, School of Medicine, Tongji University, 389 Xincun Road, Shanghai 200292, China
[5] Department of Neurology, The Affiliated Xuzhou Municipal Hospital of Xuzhou Medical University, Xuzhou No. 1 People's Hospital, 269 University Road, Xuzhou 221000, China
[6] Department of Neurology, Xuzhou Central Hospital, the Affiliated Xuzhou Clinical College of Xuzhou Medical University, 199 Jiefang South Road, Xuzhou 221000, China

Introduction

Embigin (EMB), a member of the immunoglobulin superfamily, was first identified in mouse embryonic cancer stem cells and contains a V-like domain near its transmembrane region [1]. EMB participates in various cell–cell and cell–matrix interactions, influencing processes such as cell adhesion and neuromuscular junction formation [2–5]. Despite its well-known roles in normal cells, the function of EMB in tumor progression has been less explored. In pancreatic cancer, EMB promotes invasion and migration through the induction of epithelial-mesenchymal transition (EMT) [6]. In prostate cancer, EMB enhances tumor progression by inhibiting AMP-activated protein kinase (AMPK) activity and activating nuclear factor kappa-B (NF-κB) and mechanistic target of rapamycin complex 1 (mTORC1) signaling pathways [7]. These findings suggest that EMB may facilitate tumor progression through multiple pathways.

Glioblastoma multiforme (GBM) is the most lethal tumor in the central nervous system, currently, there is still a lack of effective treatment methods [8, 9]. Our bioinformatics analysis indicates that EMB is a risk factor for GBM progression and is associated with metabolic processes within the tumor. Like its homolog basigin (BSG), EMB interacts with members of the monocarboxylate transporter (MCT) family to promote conformational changes and their transport to the plasma membrane [6]. MCT family members, such as MCT4, are critical lactate transporters that regulate aerobic glycolysis in cancer cells [10, 11]. Aerobic glycolysis is a main carbon metabolism pathway in tumor cells and is also key for energy metabolism in glioblastoma multiforme (GBM), suggesting that MCT4 may interact with EMB to affect the glycolysis metabolism of GBM [12–14].

Previous studies have shown that inhibiting EMB can decrease glycolysis levels and reduce intracellular glutathione (GSH) [15, 16]. GSH is a vital component of the cellular redox system and plays a key role in tumor cell proliferation and drug resistance. Disrupting GSH balance leads to cancer cell death through various mechanisms [17]. Glutathione peroxidase 3 (GPX3) is an important antioxidant enzyme involved in maintaining GSH redox balance, the abnormal expression of GPX3 in tumors may promote drug resistance [17]. However, currently its role in GBM is not well understood.

GBM has high resistance to chemotherapy drugs such as temozolomide (TMZ), while Chinese herbal extracts have been proven to have great potential in the treatment of GBM and may be an effective method to address GBM drug resistance [18, 19]. Ganxintriol A is a newly confirmed compound extracted from the traditional Chinese herb *Salvia przewalskii Maxim*, with a molecular formula of $C_{18}H_{16}O_6$ and an unsaturation of 11. Other extracts of *Salvia przewalskii Maxim* or *Salvia miltiorrhiza* of the same genus are reported to have anti-inflammatory, anti angiogenic, and anti-tumor effects [20–23]. At the same time, the extracts of *Salvia przewalskii Maxim* can easily pass through the blood–brain barrier and produce therapeutic effects on neurological disorders, demonstrating the Ganxintriol A's treatment potential for central nervous system tumors [24–26]. However, its role in GBM therapy has not yet been explored.

In this study, we show that EMB promotes GBM progression by enhancing EMT, intracellular glycolysis, and GSH redox balance through downstream targets MCT4 and GPX3. Furthermore, we demonstrate that Ganxintriol A acts as a potent EMB inhibitor, with significant anti-tumor effects in both in vitro and in vivo models. Our findings suggest that EMB is a valuable prognostic marker and that Ganxintriol A holds promise as a therapeutic agent for GBM.

Materials and methods

Patient tissue sample collection

Clinical GBM samples were collected from the Affiliated Hospital of Xuzhou Medical University. A total of 8 cases grade IV GBM samples, confirmed through pathological diagnosis, were included. Prior to their operations, patients had not undergone chemoradiotherapy. As a control, 4 cases of non-tumor brain tissues were acquired from patients with acute brain injuries undergoing intracranial decompression.

Cell culture and treatment

A172, U87 and LN229 cell lines were purchased from the cell bank of the Chinese Academy of Sciences. A172, U87 and LN229 cells were cultured in high glucose Dulbecco's modified Eagle's medium (DMEM) (Gibco, USA), supplemented with 10% fetal bovine serum (FBS) (Gibco, USA) and 1% penicillin–streptomycin (Beyotime, China), at 37 °C in a 5% CO_2 atmosphere.

For TMZ treatments, cells were exposed to 100 μM TMZ in high-glucose DMEM. Lentiviruses (Genechem, China) were utilized to establish control, EMB overexpression, and EMB knockdown cell lines. For VB124 treatments, cells were treated with high glucose DMEM medium containing 10 μM VB124. For Ganxintriol A treatments, cells were treated with high glucose DMEM medium containing 15 μM Ganxintriol A.

The siRNA sequences of GPX3 were: GGCAUAAGU GGCACCAUUUTTAAAUGGUGCCACUUAUGCCTT.

mRNA extraction and qRT-PCR

Total RNA was extracted using the TRIzol method (Invitrogen, USA). The extracted RNA was then reverse transcribed into cDNA using the Vic qRT Super Kit (Vicmed,

China). Real-time quantitative PCR was conducted on a LightCycler 480 system (Roche, USA), adhering to the manufacturer's protocols. GAPDH expression served as an internal reference. The expression levels of target genes in each sample were quantified using the $2^{-\Delta\Delta Ct}$ method. The primer sequences used were as follows: EMB forward, 5'-TCTCACATGCCAGTTCACAAC ATC; EMB reverse, 5'-AACACCAACAGGAACCTT TACACTC;

SLC16A3 forward, 5'-CGCCTTCCTGCTCACCAT CC; SLC16A3 reverse, 5'-GCTGAAGAGGTAGACGGA GTAGG;

E-CAD forward, 5'-GCCATCGCTTACACCATC CTCAG; E-CAD reverse, 5'-CTCTCTCGGTCCAGC CCAGTG;

N-CAD forward, 5'-AGGAGTCAGTGAAGGAGT CAGCAG; N-CAD reverse, 5'-TTCTGGCAAGTTGAT TGGAGGGATG;

GAPDH forward, 5'-TGACTTCAACAGCGACAC CCA; GAPDH reverse, 5'-CACCCTGTTGCTGTAGCC AAA.

Protein extraction and western blot

For protein extraction, 1×10^6 cells were lysed at 4 °C for 30 min using 1 mL of lysis buffer, which included protease and phosphatase inhibitors (Beyotime, China). The supernatant was then collected by centrifugation at 12,000 rpm for 30 min. Proteins were separated via gel electrophoresis and subsequently transferred to a membrane through electrophoresis. The membrane was blocked with blocking reagent (Beyotime, China) for 15 min, washed thrice with washing buffer, and incubated overnight with the primary antibody. Following this, the membrane was washed and incubated with a fluorescently tagged secondary antibody for 2 h. After a final wash, the membrane was scanned to analyze the band intensities.

Quantification of cellular GSH and 4-HNE

To quantify cellular glutathione (GSH) levels and 4-hydroxynonenal (4-HNE) levels, detection kits (Jiancheng, China) (Jianglaibio, China) was employed according to the manufacturer's guidelines. Treated cells were harvested, and the cell pellet volume was estimated visually. Four volumes of phosphate-buffered saline (PBS) were added for cell resuspension, and an ultrasonic cell crusher was used for cell disruption. In a 96-well plate, the cell lysate and detection reagents were added following the manufacturer's instructions. The contents were mixed, and the absorbance at 405 nm was measured using a microplate reader.

Quantification of glycolysis and lactate levels

Glucose uptake level and lactate level in GBM cell lines and tissues were quantified using glucose uptake assay kits (DOJINDO, Japan) and lactate assay kits (Jiancheng, China), following the manufacturer's instructions. Relative glucose uptake level and lactate level were determined based on standard curves derived from standard samples.

Assays of cell proliferation, inhibition and apoptosis

Cell proliferation was assessed using cell counting kit-8 (CCK8) assay and clone formation assay. For the CCK8 assay, cells were seeded in 96-well plates at a density of 1×10^4 cells/well. After treatment for 12 h, 24 h or 48 h, 20 μL of CCK8 reagent (Vicmed, China) was added to each well. The plates were incubated in the dark for 30 min, and absorbance at 450 nm was measured using a microplate reader.

For the clone formation assay, 1000 cells were seeded into each plate of 6-well plate and cultured ini a 5% CO_2 and 37 °C atmosphere. After treatment for 7–10 days, terminated the culture, washed and fixed the cells, then added 2 mL of 0.1% crystal violet (Vicmed, China) and stained for 15 min. The clone number was counted under the microscope.

Cell inhibition and apoptosis were evaluated using CCK8 and flow cytometry assay. For the CCK8 assay, cells were seeded in 96-well plates at a density of 1×10^4 cells/well and treated for 12 h, 24 h and 48 h. Post-treatment, 20 μL of CCK8 reagent (Vicmed, China) was added to each well, incubated in the dark for 30 min, and absorbance at 450 nm was measured.

For the flow cytometry assay, after 24 h of treatment, cells were digested, centrifuged, and resuspended in PBS. FITC-Annexin V staining solution (Keygen, China) was added to the cell suspension, mixed, and incubated for 15 min. Subsequently, PI staining solution (Keygen, China) was added, mixed again, and incubated for an additional 15 min before flow cytometry analysis.

Assays of cell invasion and migration

Cell invasion was evaluated using a transwell invasion assay. Matrix glue (Corning, USA) was diluted and added to the upper chamber of a transwell apparatus. Cells were suspended in serum-free medium and seeded in the upper chamber. The lower chamber contained medium with 20% FBS. After 24 h, cells were fixed, stained with 0.1% crystal violet (Vicmed, China), and non-invading cells were removed. Invading cells were observed, photographed, and counted.

Cell migration was assessed using transwell migration assay and wound healing assay. For the transwell

migration assay, cells were suspended in medium with 20% FBS and seeded in the upper chamber, and counted the number of migration cells to the lower chamber after 24 h. For the wound healing assay, cells were seeded in 6-well plates (Corning, USA) at a density of 1×10^5 cells/well. A scratch was created with a pipette tip, and cells were cultured in serum-free medium. The wound healing area was observed under a microscope after 24 h.

In vivo experiments

Male BALB/C nude mice (6 weeks old, 18–22 g) were acquired from Weitong Lihua Experimental Animal Technology Co., Ltd., (Beijing, China), and housed in a pathogen-free environment. During the study, they were randomly divided into groups (n = 5 per group).

For tumorigenesis experiments, 1×10^6 U87 cells were injected into the armpits of mice. Two weeks post-tumor formation, mice received intraperitoneal injections of Ganxintriol A (10 mg/kg body weight) every other day. Tumor size was measured every 4 days using the formula: $(\text{length})\times(\text{width})^2/2$. After 4 weeks, mice were humanely euthanized, and tumors were harvested.

IHC staining and IF staining

For the immunohistochemical staining, formalin-fixed, paraffin-embedded subcutaneous tumor sections were dewaxed and rehydrated. Antigen retrieval was performed by boiling in 10 mM sodium citrate buffer (Beyotime, China) (pH 6.0). Sections were incubated with primary antibodies (Abcam, USA), followed by biotinylated secondary antibodies (Abcam, USA). Slides were then immersed sequentially in horseradish peroxidase and 3,3'-diaminobenzidine (DAB) solutions (Beyotime, China), counterstained with hematoxylin (Beyotime, China), dehydrated, and sealed with neutral glue.

For the immunofluorescence staining, formalin-fixed, paraffin-embedded subcutaneous tumor sections were dewaxed, rehydrated and antigen repaired. Then incubated with the primary antibody (Abcam, USA) at 4 °C overnight. After incubation, sections were washed and incubated with a fluorescent secondary antibody (Abcam, USA) for 1 h. The cell nucleus was stained with DAPI (Beyotime, China) for 15 min, and sections were visualized using a fluorescence microscope.

Patient data and bioinformatics analyses

Data from the Human Protein Atlas (http://proteinatlas.org/), GEPIA2 (http://gepia2.cancer-pku.cn/#index), Oncomine, STRING (https://cn.string-db.org/), LinkedOmics (https://www.linkedomics.org/) and CGGA (http://www.cgga.org.cn/) databases were used to investigate EMB-related information [27–33]. GO and KEGG analyses were performed with R software (https://www.r-project.org/).

Statistical analysis

Data were analyzed using SPSS 22.0 or GraphPad Prism 8 and expressed as mean ± standard deviation. The Shapiro–Wilk normality test, with a normality rejection threshold of $P<0.05$, was used to assess data normality. Student's t-tests and one-way ANOVA were applied to determine group differences. Kaplan–Meier survival analysis and the log-rank test were used to estimate and compare survival distributions, respectively. A two-sided P-value < 0.05 was considered statistically significant.

Results

EMB is highly expressed in GBM and correlates with patient prognosis

We first analyzed EMB expression in various human tissue. As shown (Fig. 1A), EMB exhibited the highest RNA expression levels in bone marrow, lymph nodes, and small intestines, while its expression in the pancreas and skeletal muscle was comparatively low, indicating tissue-specific expression patterns.

In GBM tissue, EMB levels were approximately 2.5 times higher than those in neural stem cells and about twice as high as those in whole brain tissue, and EMB expression was the highest in GBM compared to other brain tumors, such as astrocytoma, mixed glioma, and oligodendroglioma, suggesting a correlation between EMB expression and glioma malignancy (Fig. 1D). We then examined whether EMB expression was linked to tumor stage and prognosis. Our analysis showed that high EMB levels were significantly negatively correlated with overall survival (OS) and disease-free survival (DFS) in glioma patients, indicating that EMB may play a role in GBM progression (Fig. 1B). Furthermore, we analyzed the EMB levels in Chinese glioma patients and found that EMB mRNA levels increased with glioma grade, particularly in grade IV GBM (Fig. 1E). Methylation levels of EMB were inversely correlated with EMB expression, with higher EMB levels and lower methylation associated with poorer survival outcomes (Fig. 1G, H).

GBM with mutations in the isocitrate dehydrogenase 1 (IDH1) gene and the 1p/19q codeletion have a better prognosis. In patients with high EMB levels, the IDH1 type was more likely to be wild-type, and the 1p/19q status tended to be less codeletion, which may be one of the reasons for its poor prognosis (Fig. 1F).

To verify these findings, we measured EMB expression in normal brain and GBM tissue samples. PCR and western blot (WB) analyses confirmed high EMB expression in all eight GBM samples tested (Fig. 1I, J). In GBM cell lines, U87 and LN229 exhibited significantly higher

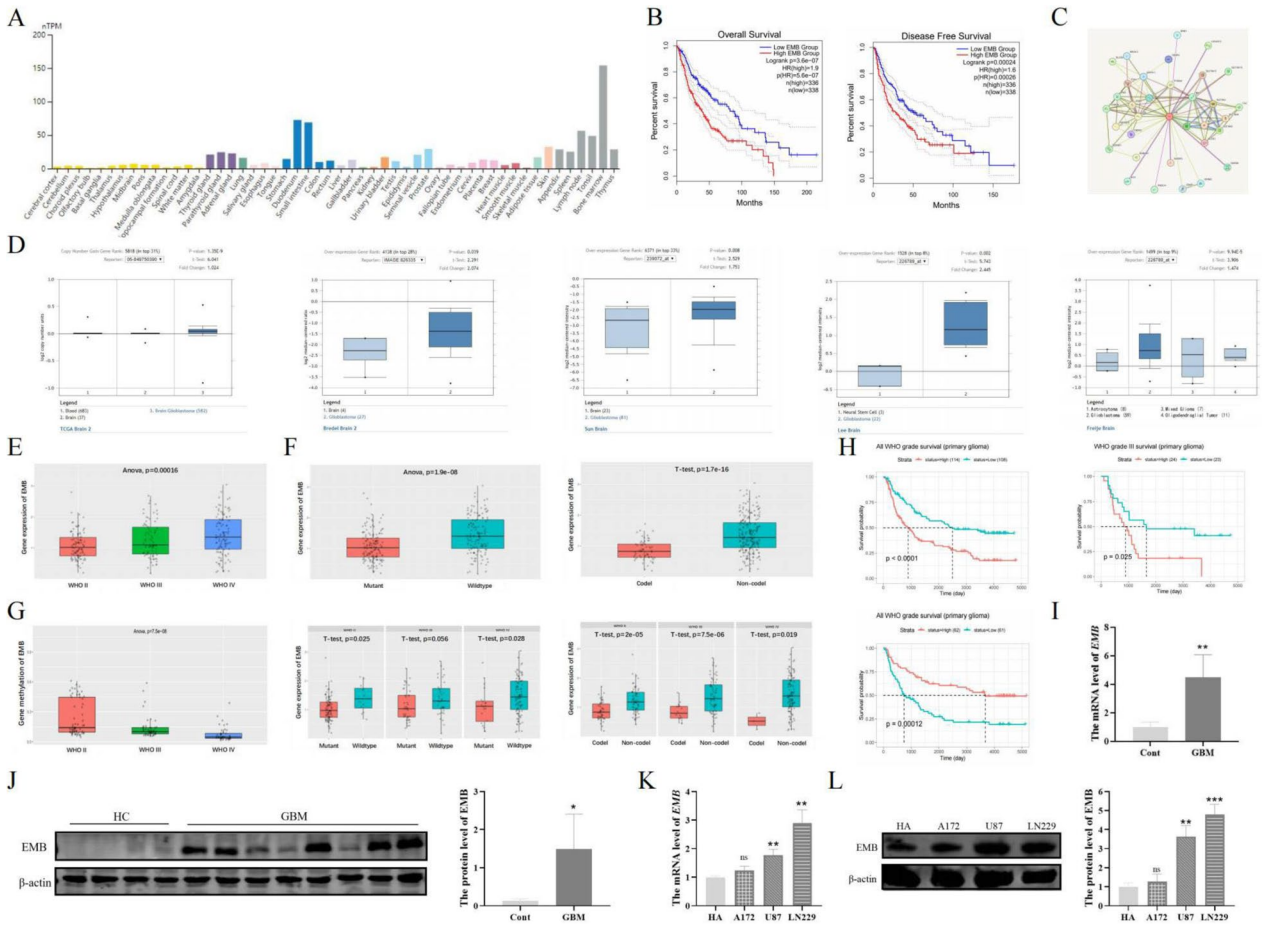

Fig. 1 EMB is highly expressed in GBM and can predict poor prognosis. **A** The expression of EMB at the mRNA level in normal human tissue. **B** The OS and DFS of glioma patient were negative relative to the expression of EMB. **C** Experimentally determined EMB-binding proteins were identified using STRING. **D** The expression of EMB in brain tumor was higher than in mormal tissue. **E** The expression of EMB in low grade glioma (LGG) and GBM. **F** EMB was more highly expressed in IDH1 wild-type glioma and 1p/19q nondeleted glioma. **G** The methylation level of EMB in LGG and GBM. **H** The patient survival was analyzed relative to the expression of EMB. **I, J** The mRNA and protein levels of EMB in patient GBM tissues were higher than in healthy tissues. **K, L** The mRNA and protein levels of EMB in cell lines. Student's t-tests and one-way ANOVA were applied to determine group differences. The data are shown as the mean ± SEM. ns $P > 0.05$, $^{*}P < 0.05$, $^{**}P < 0.01$, $^{***}P < 0.001$

EMB levels compared to normal human astrocytes (HA) (Fig. 1K, L). Based on these results, we selected U87 and LN229 cell lines for further in vitro experiments and generated EMB overexpression (oe-EMB) and knockdown (kd-EMB) models.

EMB promotes GBM cell invasion and migration via EMT

In normal tissue, EMB mediates interactions between cells and cells and the extracellular matrix. Considering the high invasiveness of GBM, we hypothesized that elevated EMB level may contribute to this phenotype. Transwell studies showed that after knocking down EMB, cells displayed reduced invasion and migration abilities, while EMB overexpression increased cell invasion and migration (Fig. 2A-D). Both invasion and migration abilities are essential for tumor metastasis. Our wound healing studies showed that EMB knockdown significantly reduced healing areas, while consistently, EMB overexpression increased healing areas in both cell models (Fig. 2E, F).

Epithelial-mesenchymal transition (EMT) is a key process in tumor invasion and metastasis, with EMT markers typically upregulated in various cancers. To investigate whether EMB influences EMT in GBM, we measured the expression of EMT-related proteins. PCR and WB analysis demonstrated that EMB overexpression increased N-cadherin (N-CAD) levels (a mesenchymal marker) and decreased E-cadherin (E-CAD) levels (an epithelial marker) in both U87 and LN229 cells. Conversely, EMB knockdown produced the

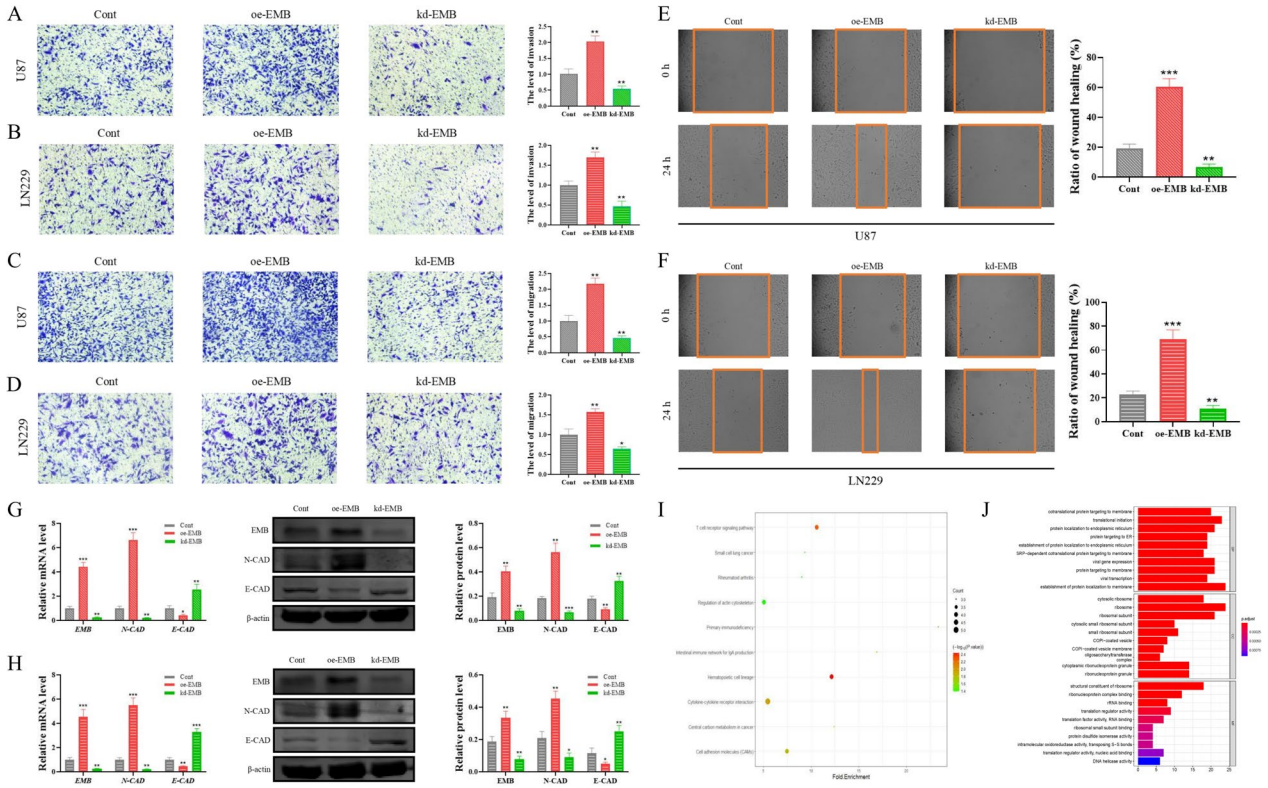

Fig. 2 EMB promotes the invasion and migration of GBM cell lines. **A**, **B** The effects of EMB on the invasion of U87 (**A**) and LN229 (**B**) cell lines were detected by transwell assays. **C**–**F** The effects of EMB on the migration of U87 (**C**, **E**) and LN229 (**D**, **F**) cell lines were detected by transwell and wound healing assays. **G, H** EMB promoted the activation of the EMT pathway in U87 (**G**) and LN229 (**H**) cells. **I**, **J** GO analyses (**I**) and KEGG pathway analyses (**J**) were performed. Student's t-tests was applied to determine group differences. The data are shown as the mean ± SEM. $^{*}P < 0.05$, $^{**}P < 0.01$, $^{***}P < 0.001$

opposite effects (Fig. 2G, H), suggesting that EMB promotes GBM cell invasion and migration through EMT activation.

EMB promotes GBM cell proliferation via MCT4-mediated glycolysis

Abnormal cell proliferation in GBM depends on high-level energy metabolism and vigorous protein synthesis. Here, we conducted bioinformatics analysis on EMB and detected several genes with the highest correlation, including SLC16A3 (the encoding gene of MCT4) (Fig. 1C). The GO and KEGG analyses showed that EMB was putatively involved in "central carbon metabolism", "protein processing in the endoplasmic reticulum" and "metabolic pathways" in tumors (Fig. 2I, J). These data putatively indicated that EMB may promote tumor proliferation via the aforementioned pathways. To clarify EMB function, we measured GBM cell proliferation levels through CCK8 and colony formation assays. The results showed that EMB overexpression significantly increased cell proliferation, while EMB knockdown led to a marked reduction in proliferation (Fig. 3A-E).

Aerobic glycolysis is a main metabolic pathway in central carbon metabolism and an important energy metabolism pathway in GBM. Here, we checked the glycolysis level of GBM cell lines and found that EMB could induce the cellular glycolysis level in GBM cells (Fig. 3F, G). The WB results showed that EMB overexpression induced MCT4 expression in U87 and LN229 cells, while EMB knockdown suppressed it (Fig. 3H-K). To confirm that MCT4 mediates the effects of EMB on GBM proliferation, we treated cells overexpressing EMB with the MCT4 inhibitor VB124. The inhibition of MCT4 reversed the increase in proliferation and glycolysis induced by EMB overexpression, indicating that EMB promotes GBM proliferation through MCT4-mediated glycolysis (Fig. 3L-Q).

EMB inhibits GBM drug resistance via GPX3

Increased glycolysis not only promotes tumor proliferation but also contributes to chemotherapy resistance. We hypothesized that elevated EMB expression was putatively related to drug resistance in GBM. Using CCK8 and flow cytometry assays, we assessed the

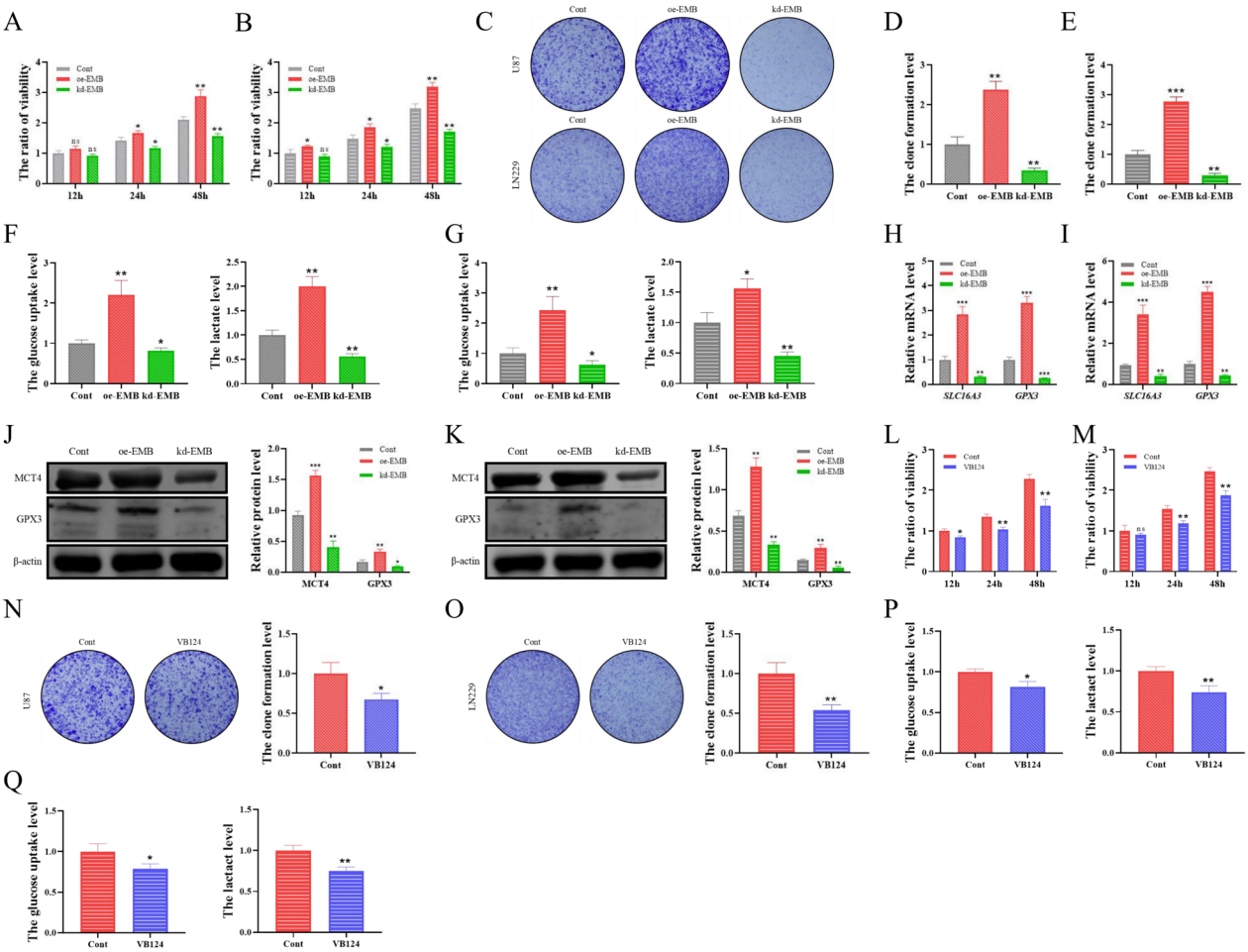

Fig. 3 The expression level of EMB is positively correlated with the proliferation and glycolysis level of GBM cells. **A**–**E** The proliferation levels of U87 (**A**, **D**) and LN229 (**B**, **E**) cells transfected with lentivirus were detected by CCK8 and clone formation assays. **F**, **G** The levels of glucose uptake and lactate of U87 (**F**) and LN229 (**G**) cells were detected. **H**–**K** The mRNA and protein levels of MCT4 and GPX3 in U87 (**H**, **J**) and LN229 (**I**, **K**) cells were detected. **L**–**O** The proliferation levels of U87 (**L**, **N**) and LN229 (**M**, **O**) oe-EMB cells treated with VB124 were decreased. **P**, **Q** The levels of glucose uptake and lactate of U87 (**P**) and LN229 (**Q**) oe-EMB cells treated with VB124 were decreased. Student's t-tests was applied to determine group differences. The data are shown as the mean ± SEM. ns $P > 0.05$, *$P < 0.05$, **$P < 0.01$, ***$P < 0.001$

effects of EMB on GBM resistance to TMZ. Our results showed that EMB-overexpressing cells had lower inhibition rates and apoptosis level, while EMB knockdown cells displayed a poor tolerance to TMZ, thereby suggesting that EMB induced drug resistance (Fig. 4A–D). The GSH redox system is an important detoxifying enzyme system and is closely linked to glycolysis. To investigate the regulatory role of EMB in GBM drug resistance, we assayed GSH and 4-hydroxynonenal (4-HNE) levels in cells and observed that EMB overexpression increased GSH levels but decreased 4-HNE levels, while EMB knockdown led to elevated oxidative stress (Fig. 4E, F).

We further nvestigated the role of GPX3, which is downstream of EMB (Fig. 4G, H). As a member of the GSH peroxidase family, its role in GBM drug resistance remains unknown. Using GPX3 small interfering RNA (siRNA) in U87 and LN229 cells, we observed a significant downregulation of drug resistance (Fig. 4I, J). As we hypothesized, interference with GPX3 leads to redox imbalance in GBM (Fig. 4K, L). These results suggest that EMB promotes drug resistance in GBM through GPX3-mediated regulation of GSH redox balance.

To investigate whether EMB promoted GBM drug resistance via GPX3, we treated GBM cells overexpressing EMB with GPX3 siRNA. CCK8 showed that upon GPX3 interference, the enhanced drug resistance mediated by EMB overexpression was reversed and accompanied by imbalanced GSH levels (Fig. 4M–P).

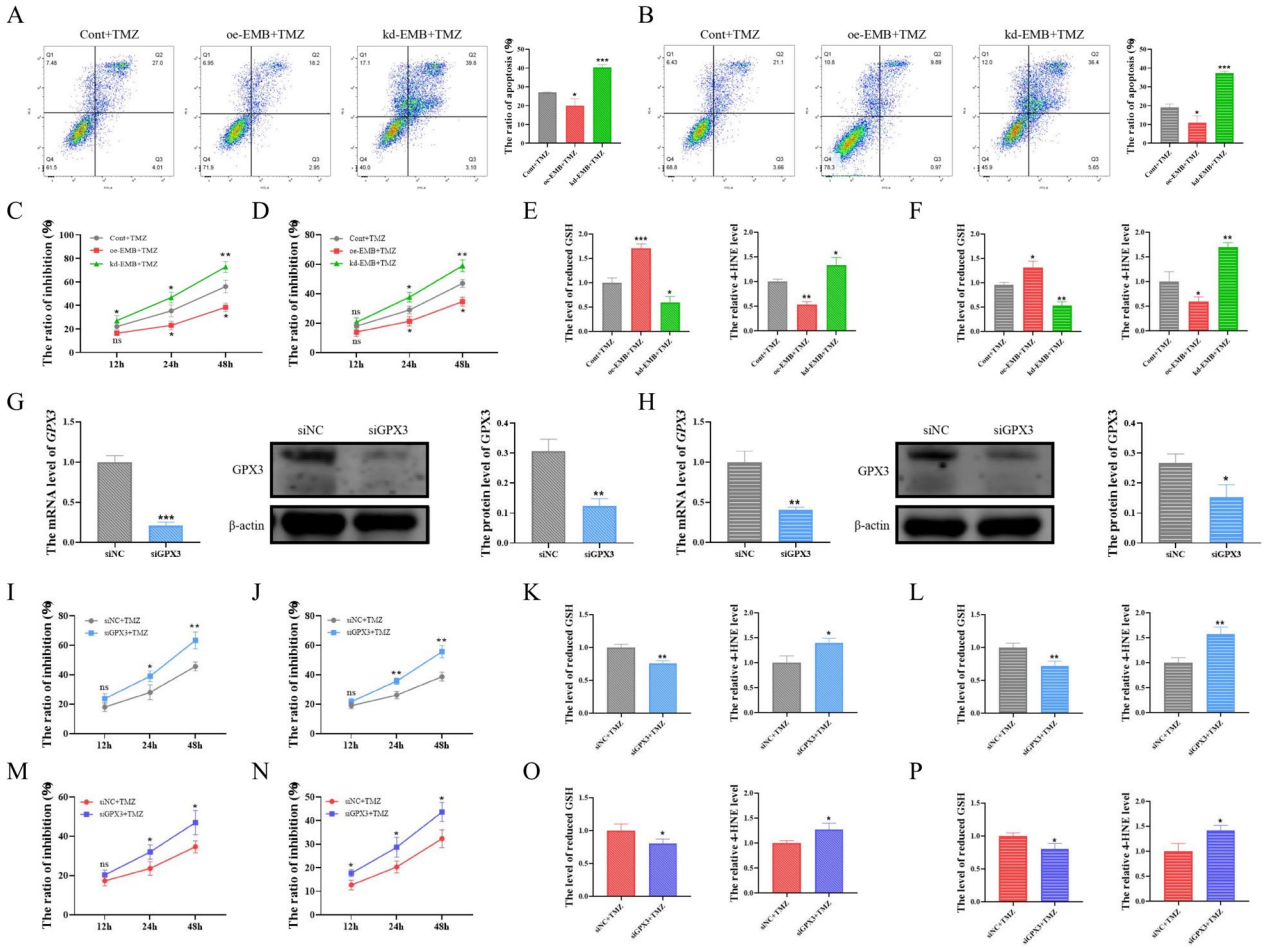

Fig. 4 Interfering with the expression of GPX3 inhibits GBM drug resistance and destroys the redox balance. **A**–**D** The apoptosis and inhibition levels of U87 (**A**, **C**) and LN229 (**B**, **D**) cells treated with TMZ were detected by flow cytometry and CCK8 assays. **E**, **F** The GSH and 4-HNE levels in U87 (**M**) and LN229 (**N**) cells treated with TMZ were detected. **G**, **H** The mRNA and protein levels of U87 (**G**) and LN229 (**H**) cells transfected with si-GPX3. **I**, **J** The inhibition levels of U87 (**I**) and LN229 (**J**) si-GPX3 transfected cells treated with TMZ were increased. **K**, **L** The GSH and 4-HNE levels of U87 (**K**) and LN229 (**L**) si-GPX3 transfected cells treated with TMZ were detected. **M**, **N** The inhibition levels of U87 (**M**) and LN229 (**N**) oe-EMB cells transfected with si-GPX3 treated with TMZ were increased. **O**, **P** The GSH and 4-HNE levels of U87 (**O**) and LN229 (**P**) oe-EMB cells transfected with si-GPX3 treated with TMZ were detected. Student's t-tests was applied to determine group differences. The data are shown as the mean ± SEM. ns $P > 0.05$, *$P < 0.05$, **$P < 0.01$, ***$P < 0.001$

Ganxintriol A reduces EMB expression and inhibits GBM progression in in vitro and in vivo experiments

Next, we explored the impact of Ganxintriol A on GBM progression. Colony formation and CCK8 assays demonstrated that Ganxintriol A significantly inhibited the proliferation of GBM cells (Fig. 5A–D). Additionally, transwell and wound healing assays revealed that Ganxintriol A suppressed the invasion and migration of U87 and LN229 cells (Fig. 5E–H). Flow cytometry analysis indicated that Ganxintriol A treatment induced apoptosis in GBM cells, further suggesting its inhibitory effects on GBM progression in vitro (Fig. 5I, J). We then examined whether Ganxintriol A could reduce EMB expression in GBM cells. PCR and WB results confirmed that Ganxintriol A effectively downregulated EMB and downstream MCT4 levels in U87 and LN229 cells (Fig. 5K–N). We also investigated its effects on glycolytic metabolism and GSH redox balance, both of which were significantly disrupted following Ganxintriol A treatment (Fig. S1A-D).

To evaluate the efficacy of Ganxintriol A in vivo, we established a subcutaneous GBM xenograft model using U87 cells in nude mice. The experimental protocol is shown in Fig. 6A. After two weeks of Ganxintriol A treatment, tumor volumes in the treatment group were significantly smaller compared to the control group (Fig. 6B–D). Additionally, mice in the Ganxintriol A treatment group exhibited longer survival

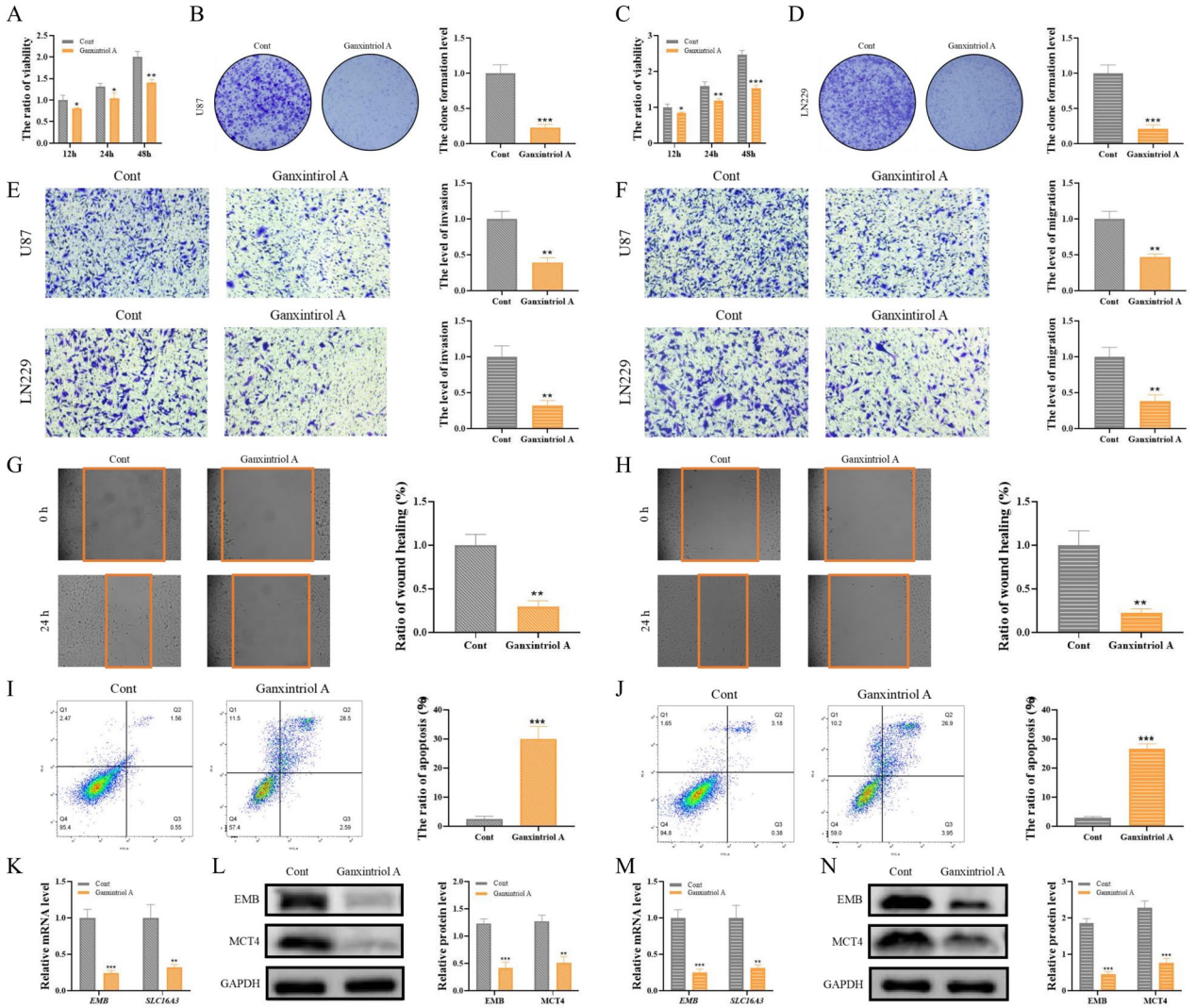

Fig. 5 Ganxintriol A down-regulates EMB expression and inhibits GBM progression in vitro. **A**–**D** The proliferation levels of U87 (**A**, **B**) and LN229 (**C**, **D**) cells treated with Ganxintriol A were detected by CCK8 and clone formation assays. **E** The invasion levels of U87 and LN229 cells treated with Ganxintriol A were decreased. **F–H** The migration levels of U87 (**G**) and LN229 (**H**) cells treated with Ganxintriol A were detected by transwell and wound healing assays. **I, J** The apoptosis levels of U87 (**I**) and LN229 (**J**) cells treated with Ganxintriol A were detected by flow cytometry. **K**–**N** The mRNA and protein levels of EMB and MVT4 in U87 (**K**, **L**) and LN229 (**M**, **N**) cells treated with Ganxintriol A were decreased. Student's t-tests was applied to determine group differences. The data are shown as the mean ± SEM. *$P < 0.05$, **$P < 0.01$, ***$P < 0.001$

times and higher body weight compared to the control group (Fig. 6E, F). Ganxintriol A treatment also caused a marked disruption in the GSH redox balance within tumors, accompanied by an increase in oxidative stress (Fig. 6G, H). Immunofluorescence staining revealed a significant reduction in EMT markers within the treated tumors (Fig. 6I, J). TUNEL and IHC staining further demonstrated that Ganxintriol A inhibited tumor proliferation and induced apoptosis in the animal models (Fig. 6K, L).

Discussion

As a newly discovered member of the immunoglobulin superfamily, EMB is primarily expressed in human prostate and breast tissues [7]. However, little research has focused on its role in cancer progression. Previous studies in pancreatic cancer suggested that EMB promotes tumor invasion and migration through the induction of EMT, while in prostate cancer, EMB activates NF-κB signaling pathways via extracellular interactions with S100A4, promoting tumor progression [6, 7]. In this study, we found that EMB is highly expressed in GBM

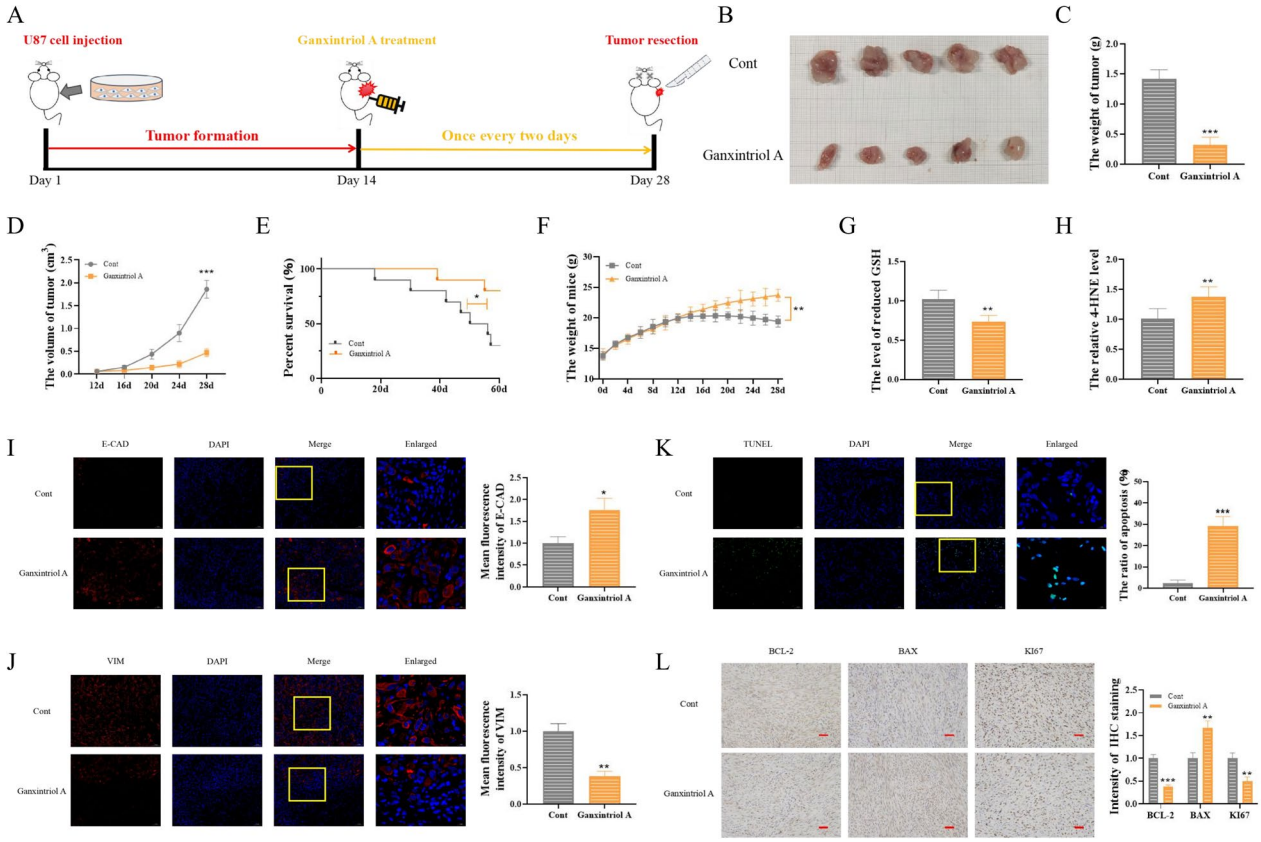

Fig. 6 Ganxintriol A inhibits GBM progression in vivo. **A** The animal experimental protocol. **B** The tumor isolated from the mice of control group and Ganxintriol A treatment group. **C**, **D** The weight (**C**) and volume (**D**) of tumors in the control group and Ganxintriol A treatment group. **E** Kaplan—Meier survival curve in the control group and Ganxintriol A treatment group of nude mice. **F** The body weight of mice in the control group and Ganxintriol A treatment group. **G**, **H** The levels of GSH (**G**) and 4-HNE (**H**) in tumors from the control group and Ganxintriol A treatment group. **I**, **J** The levels of E-CAD (**I**) and Vimentin (**J**) positive cells in tumors of the control group and Ganxintriol A treatment group. **K** The levels of TUNEL positive cells in tumors of the control group and Ganxintriol A treatment group. **L** The IHC results of the control group and Ganxintriol A treatment group. Bar = 100 μm. Student's t-tests was applied to determine group differences. Kaplan–Meier survival analysis and the log-rank test were used to estimate and compare survival distributions. The data are shown as the mean ± SEM. *$P < 0.05$, **$P < 0.01$, ***$P < 0.001$

and its expression is significantly correlated with poor prognosis in GBM patients. Gliomas with IDH mutations and 1p/19q co-deletions exhibit fewer additional genomic alterations beyond these mutations. These patients tend to benefit more from adjuvant chemotherapy and radiotherapy. Specifically, patients with high EMB levels are more likely to exhibit an IDH1 wild-type genotype and lack 1p/19q co-deletions, which are markers associated with poor glioma prognosis [34]. This suggests that EMB may play a critical role in the malignant progression of GBM. We found in our in vitro cell experiments that EMB promotes the invasion and migration of GBM cells by upregulating their EMT levels, a similar mechanism to that observed in prostate cancer [7].

It is worth noting that the uncontrolled invasion, migration, and proliferation of GBM require a significant amount of energy consumption, which is mainly supplied by aerobic glycolysis [35, 36]. Research has found that there are multiple pathways in GBM that affect cellular energy metabolism, such as KRAS/MAPK pathway, PI3K/PTEN/Akt/mTOR pathway, which are dysregulated. Targeted therapy targeting these pathways has shown promising efficacy in preclinical models, once again confirming the importance of energy metabolism in the malignant progression of GBM [37–41]. Interestingly, although EMB has not been reported to directly participate in cellular energy metabolism, it can help the lactate transporter MCT family to correctly localize the plasma membrane, thereby promoting transport of lactate through the membrane and facilitating aerobic glycolysis, providing fuel for tumor cell proliferation [42]. MCT4 has been proven to play an important role in tumor metabolism, such as in lung adenocarcinoma, MCT4 mediates immune infiltration and metabolic processes, while in pancreatic cancer, elevated MCT4 levels are associated with active glucose metabolism, leading to

increased tumor recurrence and altered cell cycle dynamics [43, 44]. Our findings showed that both glycolysis and MCT4 expression in GBM are positively regulated by intracellular EMB. This activation of EMB/MCT4-mediated glycolysis provides a potential explanation for EMB's role in promoting GBM proliferation.

Aerobic glycolysis, a key metabolic pathway in tumors, provides energy not only to support rapid cell growth and is closely linked to tumor proliferation, but also drug resistance [45, 46].The GSH redox system, which is closely linked to glycolysis, plays a major role in detoxifying cancer cells and promoting drug resistance [47–49]. For instance, GPX4 helps tumors survive by regulating ferroptosis [50]. In this study, we explored the role of GPX3 and demonstrated that EMB induces GPX3 expression. GPX3, like other members of the GPX family, reduces cellular damage by facilitating the interaction of GSH with peroxides, cell metabolites, and chemotherapeutic drugs. GPX enzymes also influence signaling pathways, mediating drug resistance through both enzymatic and non-enzymatic mechanisms [51–53]. Our findings show that knocking down GPX3 significantly reversed the drug resistance induced by EMB overexpression, accompanied by an imbalance in GSH redox levels. This indicates that EMB promotes drug resistance in GBM via downstream GPX3.

Considering that the EMB/MCT4/GPX3 axis leads to resistance of GBM to the first-line chemotherapy drug TMZ, it is of great significance to search for treatment methods to reduce tumor resistance. In recent years, an increasing number of studies have found that traditional Chinese medicine extracts exhibit significant therapeutic effects in tumor treatment, as the extracts of traditional Chinese medicine *Salvia przewalskii Maxim* have gradually been proven to have great potential in the treatment of tumors such as GBM. Previous studies have demonstrated that Tanshinone I, another extract from *Salvia przewalskii Maxim*, induces autophagy in U87 cells, while Tanshinone IIA inhibits GBM progression through the PI3K and miR-16-5p pathways [54–58]. In our study, newly identified *Salvia przewalskii Maxim* extract Ganxintriol A significantly inhibited glycolysis and disrupted redox balance in GBM cells. We hypothesize that Ganxintriol A may exert its anti-tumor effects by downregulating EMB/MCT4/GPX3 axis level. Our in vitro and in vivo experiments confirmed that Ganxintriol A treatment significantly downregulated EMB expression, suppressed tumor glycolysis, and disrupted GSH redox balance. Furthermore, Ganxintriol A reduced tumor volume and prolonged survival in GBM-bearing mice, demonstrating its therapeutic potential in GBM treatment. Based on the above findings, we summarize the specific mechanism by which Ganxintriol A inhibits GBM progression as shown in Fig. 7.

This study has some limitations that are worth discussing. Firstly, we only established a subcutaneous tumor model, which still differs from the GBM in situ model. Secondly, we were unable to delve into the mechanism by which EMB regulates changes in GPX3 expression levels, nor did we further compare the efficacy differences between Ganxintriol A and other Danshen extracts in

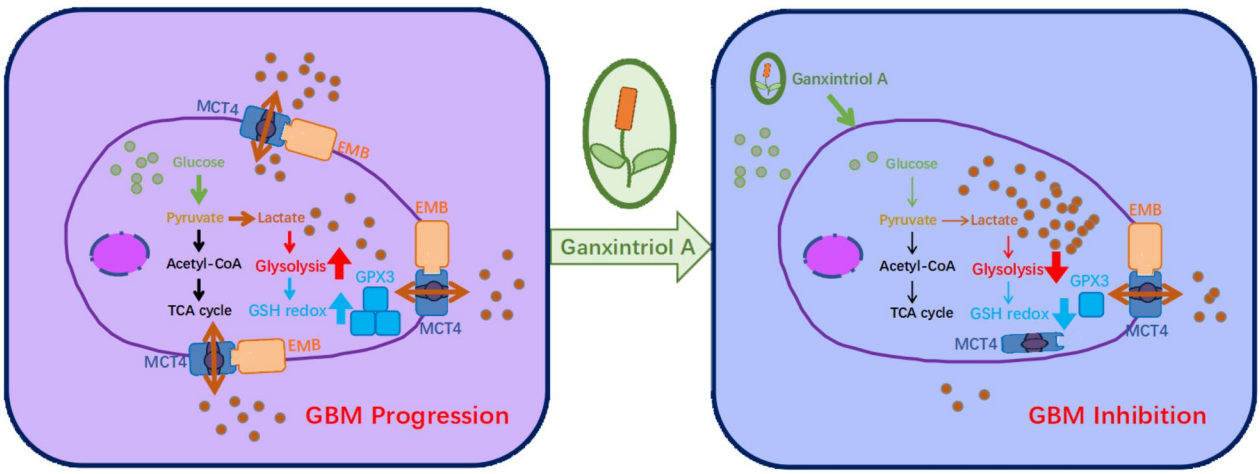

Fig. 7 Schematic diagram of Ganxintriol A inhibitors GBM progression. High levels of EMB in GBM upregulate the expression of MCT4 and promote its localization to the cell membrane, enhancing the transport of glucose and lactate in GBM cells, thereby upregulating glycolysis levels. EMB can further upregulate the expression of GPX3, thereby activating the GSH redox system, reducing oxidative stress, and promoting the survival and drug resistance of GBM. Treatment of GBM with Ganxintriol A resulted in decreased expression of EMB and MCT4, disrupting glucose and lactate transport and downregulating GPX3 expression, ultimately inhibiting the progression of GBM

GBM treatment. This will have an impact on the potential clinical applications of Ganxintriol A in the future.

Conclusion

In summary, we found that high EMB expression is associated with poor prognosis in GBM patients. The EMB/MCT4/GPX3 axis promotes GBM progression by upregulating EMT, aerobic glycolysis, and GSH redox balance. Our findings also identify Ganxintriol A, a traditional Chinese medicine extract, as a promising therapeutic agent for GBM.

Abbreviations

AMPK	AMP-activated protein kinase
BSG	Basigin
CCK8	Cell counting kit-8
DFS	Disease-free survival
E-CAD	E-cadherin
EMB	Embigin
EMT	Epithelial-mesenchymal transition
GBM	Glioblastoma multiforme
GO	Gene ontology
GPX3	Glutathione peroxidase 3
GSH	Glutathione
IDH1	Isocitrate dehydrogenase 1
kd-EMB	Knockdown EMB
KEGG	Kyoto encyclopedia of genes and genomes
MCT	Monocarboxylate transporter
MCT4	Monocarboxylate transporter 4
mTORC1	Mechanistic target of rapamycin complex 1
N-CAD	N-cadherin
NF-κB	Nuclear factor kappa-B
oe-EMB	Overexpression EMB
OS	Overall survival
qRT-PCR	Quantitative real time polymerase chain reaction
TMZ	Temozolomide
WB	Western blot
4-HNE	4-Hydroxynonenal

Supplementary Information

The online version contains supplementary material available at https://doi.org/10.1186/s12967-025-06290-z.

Supplementary Material 1: Figure S1. Ganxintriol A down-regulates glycolysis and GSH redox in vitro. A, B The levels of glucose uptake and lactate of U87 (A) and LN229 (B) cells under Ganxintriol A treatment were decreased. C, D The intracellular GSH and 4-HNE levels of U87 (C) and LN229 (D) cells were detected. Student's t-tests was applied to determine group differences. The data are shown as the mean ± SEM. *P < 0.05, **P < 0.01.

Acknowledgements

We thank Professor Zhonghai Zhou for his support of the experimental equipment. We acknowledge the Human Protein Atlas, GEPIA2, Oncomine, STRING, LinkedOmics and CGGA database for providing their platforms and contributors for uploading their meaningful datasets.

Author contributions

The conception and design of the work were prepared by Wu XJ and Cheng B. The experiment was performed by Cheng B, Liu J, Gao L and Zhu ZW, while the analysis and interpretation of data were done by Yang Y and Liu SQ. Drafting of the manuscript was done by Wu XJ and Cheng B. All the authors revised the manuscript and approved the submission. Cheng B and Liu J contributed equally to this work.

Funding

This study was supported by the project of Administration of Traditional Chinese Medicine of Jiangsu Province of China (No. MS2022066), the Xuzhou Municipal Science and Technology Bureau (No. KC23220), the Xuzhou Health Commission (No. XWKYHT20220137), the Development Fund of the Affiliated Hospital of Xuzhou Medical University (No. XYFY202235), and the Affiliated Xuzhou Eastern Hospital of Xuzhou Medical University (No. 2022009).

Availability of data and materials

All data generated or analysed during this study are included in this published article.

Declarations

Ethics approval and consent to participate

The study was conducted in accordance with the Declaration of Helsinki and approved by the Institutional Review Board (or Ethics Committee) of The Affiliated Hospital of Xuzhou Medical University (XYFY2022-KL362-01). All animal experiments were approved by the Experimental Animal Ethics Committee of Xuzhou Medical University (202306T001) and conducted in accordance with relevant ethical standards and guidelines. Human Protein Atlas, GEPIA2, Oncomine, STRING, LinkedOmics and CGGA belong to public databases. The patients involved in the database have obtained ethical approval. Users can download relevant data for free for research and publish relevant articles. Our study is based on open source data, so there are no ethical issues and other conflicts of interest.

Consent for publication

Not applicable.

Competing interests

The authors declare that they have no competing interests.

Received: 21 September 2024 Accepted: 23 February 2025
Published online: 04 March 2025

References

1. Huang R, Ozawa M, Kadomatsu K, Muramatsu T. Developmentally regulated expression of embigin, a member of the immunoglobulin superfamily found in embryonal carcinoma cells. Diff Res Biol Div. 1990;45(2):76–83.
2. Huang R, Ozawa M, Kadomatsu K, Muramatsu T. Embigin, a member of the immunoglobulin superfamily expressed in embryonic cells, enhances cell-substratum adhesion. Dev Biol. 1993;155(2):307–14.
3. Tachikui H, Kurosawa N, Kadomatsu K, Muramatsu T. Genomic organization and promoter activity of embigin, a member of the immunoglobulin superfamily. Gene. 1999;240(2):325–32.
4. Muramatsu T. Cell surface glycoproteins: biochemical, immunological and molecular biological studies. Nagoya J Med Sci. 1994;57(3–4):95–108.
5. Lain E, Carnejac S, Escher P, Wilson M, Lømo T, Gajendran N, et al. A novel role for embigin to promote sprouting of motor nerve terminals at the neuromuscular junction. J Biol Chem. 2009;284(13):8930–9.
6. Jung D, Kim J, Kim C, Song S. Embigin is overexpressed in pancreatic ductal adenocarcinoma and regulates cell motility through epithelial to mesenchymal transition via the TGF-β pathway. Mol Carcinog. 2016;55(5):633–45.
7. Ruma IMW, Kinoshita R, Tomonobu N, Inoue Y, Kondo E, Yamauchi A, et al. Embigin promotes prostate cancer progression by S100A4-dependent and-independent mechanisms. Cancers (Basel). 2018;10(7):239.
8. Vaubel RA, Tian S, Remonde D, Schroeder MA, Mladek AC, Kitange GJ, et al. Genomic and phenotypic characterization of a broad panel of patient-derived xenografts reflects the diversity of glioblastoma. Clin Cancer Res. 2020;26(5):1094–104.
9. Ganapathy-Kanniappan S, Geschwind J. Tumor glycolysis as a target for cancer therapy: progress and prospects. Mol Cancer. 2013;12:152.
10. Wilson M, Meredith D, Fox J, Manoharan C, Davies A, Halestrap A. Basigin (CD147) is the target for organomercurial inhibition of monocarboxylate

transporter isoforms 1 and 4: the ancillary protein for the insensitive MCT2 is EMBIGIN (gp70). J Biol Chem. 2005;280(29):27213–21.
11. Guo C, Huang T, Wang Q, Li H, Khanal A, Kang E, et al. Monocarboxylate transporter 1 and monocarboxylate transporter 4 in cancer-endothelial co-culturing microenvironments promote proliferation, migration, and invasion of renal cancer cells. Cancer Cell Int. 2019;19:170.
12. Ke X, Fei F, Chen Y, Xu L, Zhang Z, Huang Q, et al. Hypoxia upregulates CD147 through a combined effect of HIF-1α and Sp1 to promote glycolysis and tumor progression in epithelial solid tumors. Carcinogenesis. 2012;33(8):1598–607.
13. Zhao Y, Song J, Dong W, Liu X, Yang C, Wang D, et al. The MBNL1/circNTRK2/PAX5 pathway regulates aerobic glycolysis in glioblastoma cells by encoding a novel protein NTRK2-243aa. Cell Death Dis. 2022;13(9):767.
14. Luo K, Liu A, Wu H, Liu Q, Dai J, Liu Y, et al. CircKIF4A promotes glioma growth and temozolomide resistance by accelerating glycolysis. Cell Death Dis. 2022;13(8):740.
15. Khan A, Valli E, Lam H, Scott D, Murray J, Hanssen K, et al. Targeting metabolic activity in high-risk neuroblastoma through monocarboxylate transporter 1 (MCT1) inhibition. Oncogene. 2020;39(17):3555–70.
16. Perez-Escuredo J, Van Hee VF, Sboarina M, Falces J, Payen VL, Pellerin L, et al. Monocarboxylate transporters in the brain and in cancer. Biochem Biophys Acta. 2016;1863(10):2481–97.
17. Traverso N, Ricciarelli R, Nitti M, Marengo B, Furfaro AL, Pronzato MA, et al. Role of glutathione in cancer progression and chemoresistance. Oxid Med Cell Longev. 2013;2013: 972913.
18. Sun T, Lin B, Sun Q, Zhang X, Wang T, Yang J, et al. Gambogic acid impairs the maintenance and therapeutic resistance of glioma stem cells by targeting B-cell-specific Moloney leukemia virus insert site 1. Phytomedicine. 2024;135: 156070.
19. Zhu S, Guo J, Yu L, Liu J, Chen J, Xin J, et al. Synergistic effect of cryptotanshinone and temozolomide treatment against human glioblastoma cells. Sci Rep. 2023;13:21835.
20. Ke F, Wang Z, Song X, Ma Q, Hu Y, Jiang L, et al. Cryptotanshinone induces cell cycle arrest and apoptosis through the JAK2/STAT3 and PI3K/Akt/NFκB pathways in cholangiocarcinoma cells. Drug Des Devel Ther. 2017;11:1753–66.
21. Bai J, Qin Q, Li S, Cui X, Zhong Y, Yang L, et al. Salvia miltiorrhiza inhibited lung cancer through aerobic glycolysis suppression. J Ethnopharmacol. 2024;331: 118281.
22. Cai P, Sheng G, Jiang S, Wang D, Zhao Z, Huang M, et al. Comparative proteomics analysis reveals the reversal effect of cryptotanshinone on gefitinib-resistant cells in epidermal growth factor receptor-mutant lung cancer. Front Pharmacol. 2022;13: 837055.
23. Qiu B, Wang P, Li J. Salvia przewalskii Salprzesides A and B: two novel icetexane diterpenes with antiangiogenic activity from Maxim. Nat Prod Res. 2022;36:2479–85.
24. Wang H, Zhang M, Fang J, He Y, Liu M, Hong Z, et al. *Salvia miltiorrhiza* simultaneous determination of seven lipophilic and hydrophilic components in bunge by LC-MS/MS method and its application to a transport study in a blood-brain-barrier cell model. Molecules. 2022;27(3):657.
25. Subedi L, Gaire BP. Tanshinone IIA: a phytochemical as a promising drug candidate for neurodegenerative diseases. Pharmacol Res. 2021;169: 105661.
26. Zhang T, Pan W, Tan X, Yu J, Cheng S, Wei S, et al. A novel L-shaped orthoquinone analog suppresses glioblastoma progression by targeting acceleration of AR degradation and regulating PI3K/AKT pathway. Biochem Pharmacol. 2024;226: 116398.
27. The Human Protein Atlas. Sweden. http://proteinatlas.org/. Accessed 22 Jun 2024.
28. Uhlén M, Fagerberg L, Hallström BM, Lindskog C, Oksvold P, Mardinoglu A, et al. Proteomics. Tissue-based map of the human proteome. Science. 2015;347:1260419.
29. Zefang T, Boxi K, Chenwei L, et al. GEPIA2: an enhanced web server for large-scale expression profiling and interactive analysis. Nucleic Acids Res. 2019;47:W556–60.
30. STRING, Protein network of EMB, https://cn.string-db.org/cgi/network?taskId=beJ1VXVeDkfC&sessionId=bQz7I0J6EzEr, Accessed 15 Sep 2024.
31. Vasaikar S, Straub P, Wang J, Zhang B. LinkedOmics: analyzing multi-omics data within and across 32 cancer types. Nucleic Acids Res. 2018;46:D956–63.
32. Zhao Z, Zhang KN, Wang Q, Li G, Zeng F, Zhang Y, et al. Chinese glioma genome atlas (CGGA): a comprehensive resource with functional genomic data from chinese glioma patients. GPB. 2021;19(1):1–12.
33. The Human Protein Atlas, Brain single cell expression of EMB, https://www.proteinatlas.org/ENSG00000170571-EMB/tissue, Accessed 22 Jun 2024.
34. Eckel-Passow JE, Lachance DH, Molinaro AM, Walsh KM, Decker PA, Sicotte H, et al. Glioma groups based on 1p/19q, IDH, and TERT promoter mutations in tumors. N Engl J Med. 2015. https://doi.org/10.1056/NEJMoa1407279.
35. Duraj T, Kalamian M, Zuccoli G, Maroon JC, D'Agostino DP, Scheck AC, et al. Clinical research framework proposal for ketogenic metabolic therapy in glioblastoma. BMC Med. 2024;22:578.
36. Zhou Z, Yin X, Sun H, Lu J, Li Y, Fan Y, et al. PTBP1 lactylation promotes glioma stem cell maintenance through PFKFB4-driven glycolysis. Cancer Res, 2024, undefined.
37. Köpnick A, Geistlinger K, Beitz E. Cysteine 159 delineates a hinge region of the alternating access monocarboxylate transporter 1 and is targeted by cysteine-modifying inhibitors. FEBS J. 2021;288(20):6052–62.
38. Sun X, Wang M, Wang M, Yao L, Li X, Dong H, et al. Role of proton-coupled monocarboxylate transporters in cancer: from metabolic crosstalk to therapeutic potential. Front Cell Dev Biol. 2020;8:651.
39. Mukhopadhyay S, Vander Heiden MG, McCormick F. The metabolic landscape of RAS-driven cancers from biology to therapy. Nat Cancer. 2021;2:271–83.
40. Holmen SL, Williams BO. Essential role for Ras signaling in glioblastoma maintenance. Cancer Res. 2005;65:8250–5.
41. Mao H, Lebrun DG, Yang J, Zhu VF, Li M. Deregulated signaling pathways in glioblastoma multiforme: molecular mechanisms and therapeutic targets. Cancer Invest. 2012;30:48–56.
42. Halestrap AP. The SLC16 gene family - structure, role and regulation in health and disease. Mol Aspects Med. 2013;34(2–3):337–49.
43. Ren W, Yuan Y, Chen X, Zhai H, An Y, Tang L, et al. Identification and validation of long non-coding RNA LCIIAR as a biomarker in LUAD. Front Oncol. 2022;12: 933071.
44. Lee S, Hwang H, Lee W, Kang C. MCT4 as a potential therapeutic target to augment gemcitabine chemosensitivity in resected pancreatic cancer. Cell Oncol. 2021;44(6):1363–71.
45. Feng Z, Ou Y, Hao L. The roles of glycolysis in osteosarcoma. Front Pharmacol. 2022;13: 950886.
46. Pi M, Kuang H, Yue C, Yang Q, Wu A, Li Y, et al. Targeting metabolism to overcome cancer drug resistance: a promising therapeutic strategy for diffuse large B cell lymphoma. Drug Resist Updat. 2022;61: 100822.
47. Lin H, Lim S, Hsu T, Yang W, Huang C, Tsai Y, et al. CCAAT/enhancer-binding protein delta regulates glioblastoma survival through catalase-mediated hydrogen peroxide clearance. Oxid Med Cell Longev. 2022;2022:4081380.
48. Zhu Z, Du S, Du Y, Ren J, Ying G, Yan Z. Glutathione reductase mediates drug resistance in glioblastoma cells by regulating redox homeostasis. J Neurochem. 2018;144(1):93–104.
49. Oancea-Castillo LR, Klein C, Abdollahi A, Weber KJ, Regnier-Vigouroux A, Dokic I. Comparative analysis of the effects of a sphingosine kinase inhibitor to temozolomide and radiation treatment on glioblastoma cell lines. Cancer Biol Ther. 2017;18(6):400–6.
50. Kram H, Prokop G, Haller B, Gempt J, Wu Y, Schmidt-Graf F, et al. Glioblastoma Relapses Show Increased Markers of Vulnerability to Ferroptosis. Front Oncol. 2022;12: 841418.
51. Zhang ML, Wu HT, Chen WJ, Xu Y, Ye QQ, Shen JX, et al. Involvement of glutathione peroxidases in the occurrence and development of breast cancers. J Transl Med. 2020;18(1):247.
52. Huang Y, Fang W, Wang Y, Yang W, Xiong B. Transforming growth factor-β1 induces glutathione peroxidase-1 and protects from H2O2-induced cell death in colon cancer cells via the Smad2/ERK1/2/HIF-1α pathway. Int J Mol Med. 2012;29(5):906–12.
53. Mouret S, Sauvaigo S, Peinnequin A, Favier A, Beani JC, Leccia MT. E6* oncoprotein expression of human papillomavirus type-16 determines different ultraviolet sensitivity related to glutathione and glutathione peroxidase antioxidant defence. Exp Dermatol. 2005;14(6):401–10.
54. Jian S, Chen L, Minxue L, Hongmin C, Ronghua T, Xiaoxuan F, et al. Tanshinone I induces apoptosis and protective autophagy in human

glioblastoma cells via a reactive oxygen species-dependent pathway. Int J Mol Med. 2020;45:983–92.
55. Schaf J, Shinhmar S, Zeng Q, Pardo OE, Beesley P, Syed N, et al. Enhanced sestrin expression through tanshinone 2A treatment improves PI3K-dependent inhibition of glioma growth. Cell Death Discov. 2023;9:172.
56. You S, He X, Wang M, Mao L, Zhang L. Tanshinone IIA suppresses glioma cell proliferation, migration and invasion both in vitro and in vivo partially through miR-16-5p/Talin-1 (TLN1) axis. Cancer Manag Res. 2020;12:11309–20.
57. Zhong B, Yu J, Hou Y, Ai N, Ge W, Lu JJ, et al. A novel strategy for glioblastoma treatment by induction of noptosis, an NQO1-dependent necrosis. Free Radic Biol Med. 2021;166:104–15.
58. Qi H, Chen Z, Qin Y, Wang X, Zhang Z, Li Y. Tanshinone IIA inhibits cell growth by suppressing SIX1-induced aerobic glycolysis in non-small cell lung cancer cells. Oncol Lett. 2022;23:184.

Publisher's Note